AFRL-AFOSR-VA-TR-2023-0139

Chemical Reactions of Cold Molecular Ions and Molecular Radicals

Lewandowski, Heather
REGENTS OF THE UNIVERSITY OF COLORADO
3100 MARINE ST 572 UCB
BOULDER, CO,
US

11/03/2022
Final Technical Report

Air Force Research Laboratory
Air Force Office of Scientific Research
Arlington, Virginia 22203
Air Force Materiel Command

REPORT DOCUMENTATION PAGE

PLEASE DO NOT RETURN YOUR FORM TO THE ABOVE ORGANIZATION.

1. REPORT DATE	2. REPORT TYPE	3. DATES COVERED	
20221103	Final	START DATE 20160401	END DATE 20200930

4. TITLE AND SUBTITLE
Chemical Reactions of Cold Molecular Ions and Molecular Radicals

5a. CONTRACT NUMBER	5b. GRANT NUMBER	5c. PROGRAM ELEMENT NUMBER
	FA9550-16-1-0117	61102F
5d. PROJECT NUMBER	**5e. TASK NUMBER**	**5f. WORK UNIT NUMBER**

6. AUTHOR(S)
Heather Lewandowski

7. PERFORMING ORGANIZATION NAME(S) AND ADDRESS(ES)
REGENTS OF THE UNIVERSITY OF COLORADO
3100 MARINE ST 572 UCB
BOULDER, CO
US

8. PERFORMING ORGANIZATION REPORT NUMBER

9. SPONSORING/MONITORING AGENCY NAME(S) AND ADDRESS(ES)	10. SPONSOR/MONITOR'S ACRONYM(S)	11. SPONSOR/MONITOR'S REPORT NUMBER(S)
Air Force Office of Scientific Research 875 N. Randolph St. Room 3112 Arlington, VA 22203	AFRL/AFOSR RTB2	AFRL-AFOSR-VA-TR-2023-0139

12. DISTRIBUTION/AVAILABILITY STATEMENT
A Distribution Unlimited: PB Public Release

13. SUPPLEMENTARY NOTES

14. ABSTRACT
Support from AFOSR award FA9550-16-1-0117 has enabled the investigation of new schemes to access high orbital angular momentum Rydberg states and to characterize molecular ionization dynamics relevant to the production of molecular ions in a single, selected quantum state. Our unique scheme for molecular ion production involves accessing high orbital angular momentum (â„“) core-nonpenetrating (CNP) Rydberg states, which subsequently undergo spontaneous vibrational autoionization to generate the bare ion in a single selected v, J, M quantum state. Populating these CNP Rydberg states involves traversing a region of state space where predissociation leads to rapid non-radiative decay of the target species. This universally occurring decay process in molecules necessitates coherent population transfer to avoid these lossy intermediate states, motivating our development of optical-millimeter-wave stimulated Raman adiabatic passage as detailed in previous progress reports and in several of the publications supported by this award.

15. SUBJECT TERMS

16. SECURITY CLASSIFICATION OF:			17. LIMITATION OF ABSTRACT	18. NUMBER OF PAGES
a. REPORT	b. ABSTRACT	c. THIS PAGE		
U	U	U	UU	5

19a. NAME OF RESPONSIBLE PERSON	19b. PHONE NUMBER *(Include area code)*
MICHAEL BERMAN	426-7781

Support from AFOSR award FA9550-16-1-0117 has enabled the investigation of new schemes to access high orbital angular momentum Rydberg states and to characterize molecular ionization dynamics relevant to the production of molecular ions in a single, selected quantum state. Our unique scheme for molecular ion production involves accessing high orbital angular momentum (ℓ) core-nonpenetrating (CNP) Rydberg states, which subsequently undergo spontaneous vibrational autoionization to generate the bare ion in a single selected v, J, M quantum state. Populating these CNP Rydberg states involves traversing a region of state space where predissociation leads to rapid non-radiative decay of the target species. This universally occurring decay process in molecules necessitates coherent population transfer to avoid these lossy intermediate states, motivating our development of optical-millimeter-wave stimulated Raman adiabatic passage as detailed in previous progress reports and in several of the publications supported by this award. Below, we describe theoretical and experimental progress toward implementation of our unique method for single quantum state preparation of the NO^+ molecular ion.

Vibrational autoionization of high-ℓ Rydberg states of NO

We have extended the long-range model of autoionization, initially developed by Ed Eyler to examine the linewidths of autoionizing nf Rydberg states of H_2 [1], to study vibrational autoionization in NO. This fully ab initio model allows for detailed predictions of the autoionization rate into every allowed decay channel, as a function of all quantum numbers (n, ℓ, v, R, ℓ_R). We have validated our model by measuring the total decay rates of individual ℓ_R components of the manifold of ng (v=1) Rydberg states for several values of the ion-core rotational quantum number, R. Unlike lower ℓ Rydberg states of NO, in which predissociation is orders of magnitude faster than autoionization [2], we find that the total decay rates of ng Rydberg states are consistent with our model, suggesting autoionization is the dominant non-radiative decay pathway for high-ℓ Rydberg states of NO.

Our primary motivation for the investigation of the vibrational autoionizing states is their potential utility in producing few or even single quantum states of a molecular ion. To that end, we undertook a comparison of our model predictions with the rotationally resolved photoelectron spectra of vibrationally autoionizing nf states of NO collected by the Zare group [3,5]. To our surprise, the intensity in most of the decay channels observed in the Zare group experiments could be explained by long-range autoionization. Figure 1 shows the theoretical (left bars in blue, red, and green) and experimental (right bars in teal) ion rotational state changes following $\Delta v=-1$ vibrational autoionization of the 11f (v=2, R=16, $\ell_R=-1,0,1$) Rydberg state. Intensities in all observed decay channels are reproduced by our calculation. Figure 2 shows a similar comparison for the 10f(v=2, R=18, $\ell_R=3$) Rydberg state. Although we calculate similar intensities in four of the six observed decay channels, the large ion rotational state changes ($N^+-R=3,4$) are not captured by the model. The "mirror" pattern was observed for $\ell_R=-3$ states, and again our model does not result in large ion rotational state changes ($N^+-R=-3,-4$). We are investigating extensions to our model including higher-order multipoles, higher-order polarizabilities, and hyperpolarizabilities, however, these are generally too small in magnitude to produce the observed intensities. We hypothesize that a valence state-mediated mechanism is responsible for autoionization via these pathways, since the $\ell_R=\pm3$ states of a Rydberg complex in the high rotation limit have the largest fractional sigma character in a Hund's case (b) basis. This sigma character means these states experience stronger Rydberg-valence interactions than other ℓ_R states. This "electronic" mechanism for vibrational autoionization has been frequently invoked in

the literature [3,4], but our work significantly limits the scope of possible Rydberg-valence interactions responsible for this type of decay.

Most significantly, our model allows for confident predictions of the ion rotational state distribution following vibrational autoionization of ng Rydberg states of NO, our proposed "precursor" to single quantum state molecular ions. Figure 3 shows predicted ion rotational state distributions for all ℓ_R components of the 25g (v=1) Rydberg states with R values of (a) 0, (b) 1, (c) 2, and (d) 3. These plots show that for ng (and higher ℓ) Rydberg states, dipole-mediated vibrational autoionization dominates the decay resulting in significant intensity in one or both of the $N^+-R=\pm1$ decay channels. For example, by preparing the 25g(v=1, R=0) Rydberg state of NO, vibrational autoionization will yield at least 90% of all molecular ions in the $N^+=1$ rotational level of the ground vibronic state of NO^+. Thus, vibrational autoionization of high-ℓ Rydberg states is a productive strategy for generating few or single quantum state-selected molecular ions. We look forward to expanding our work to other molecular species of interest to cold chemistry experiments.

References

[1] Eyler EE. *Phys. Rev. A.* **1986**, 34(4), 2881.

[2] Fujii A and Morita N. *J. Chem. Phys.* **1995**, 103, 6029.

[3] Park H, Leahy DJ, and Zare RN. *Phys. Rev. Lett.* **1996**, 76(10), 1591.

[4] Pratt ST. *J. Chem. Phys.* **1998**, 108, 7131.

[5] Zhao R. *PhD Thesis.* **2004**, Stanford University.

Publications supported by AFOSR

Barnum TJ, Field RW. Long-range model of vibrational autoionization in high-ℓ Rydberg states of NO. In preparation. **2020**.

Barnum TJ, Herburger H, Grimes DD, Jiang J, Field RW. Preparation of high orbital angular momentum Rydberg states by optical-millimeter-wave STIRAP. Submitted to J. Chem. Phys. **2020**.

Jiang J, Du Z, Liéven J, Field RW. One-colour (~220 nm) resonance-enhanced (S_1-S_0) multi-photon dissociation of acetylene: probe of the C_2 A $^1\Pi_u$ – X $^1\Sigma^+_g$ band by frequency-modulation spectroscopy. Mol. Phys. **2020**, Accepted. DOI: 10.1080/00268976.2020.1724340

Barnum TJ. Spectroscopy and dynamics of high orbital angular momentum Rydberg states. PhD Thesis. **2020**, Massachusetts Institute of Technology.

Jiang J, Du Z, Field RW. Determination of the sign of the population difference in a two-level system by frequency-modulation spectroscopy. Mol. Phys. **2020**, 118(7), e1660007.

Bergmann K, Nägerl HC, Panda C, Gabrielse G, Miloglyadov E, Quack M, Seyfang G, Wichmann G, Ospelkaus S, Kuhn A, Longhi S, Szameit A, Pirro P, Hillebrands B, Zhu X-F, Zhu J, Drewsen M, Hensinger WK, Weidt S, Halfmann T, Wang H-L, Paraoanu GS, Vitanov NV, Mompart J, Busch T, Barnum TJ, Grimes DD, Field RW, Raizen MG,

Narevicius E, Auzinsh M, Budker D, Pálffy A, Keitel CH. Roadmap on STIRAP applications. J. Phys. B. **2019**, 52(20), 202001.

Clausen G. Vibrational autoionization of high-ℓ Rydberg states of NO. B.Sc. Thesis. **2018**, ETH Zürich.

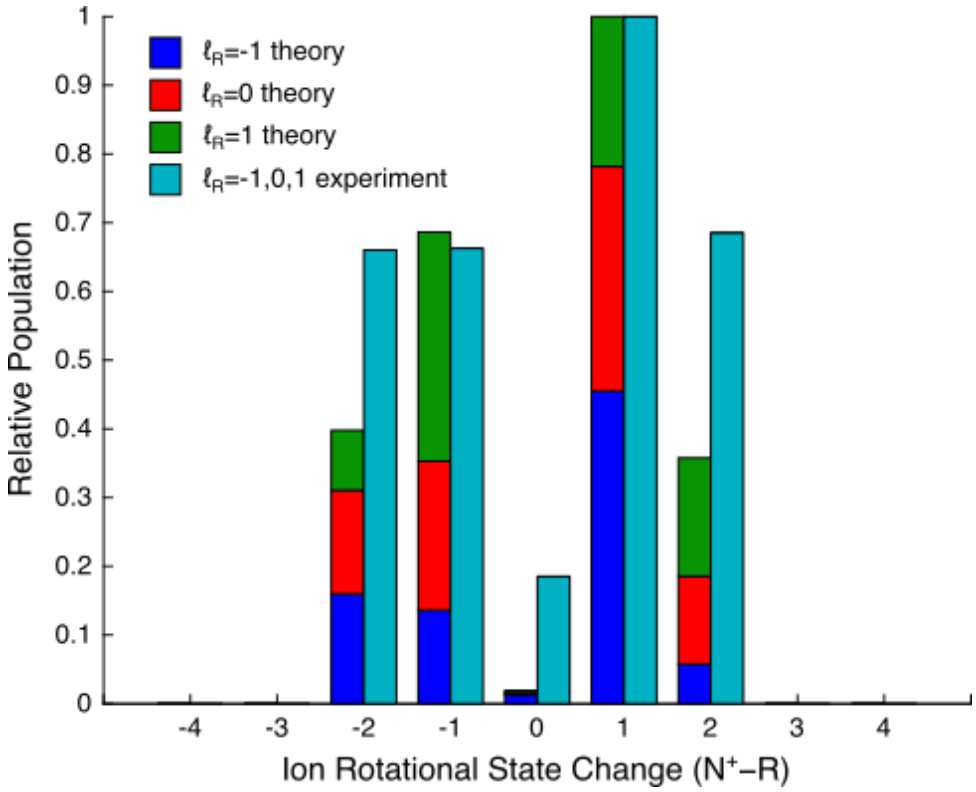

Figure 1. Rotational state change following vibrational autoionization of the 13f (v=2, R=16, ℓ_R=−1,0,1) Rydberg states. The rotational levels of the ion (N^+) are populated in the v=1 level of the ground electronic state of NO+. The experimental data are the average of the photoelectron signal intensities collected at 0° and 90° angles between the polarization vectors of the two excitation lasers. This is *not* an accurate measurement of the ion rotational distributions, but provides a useful qualitative comparison with the model. The intensity pattern in all experimentally observed decay channels is reproduced by the long-range calculation.

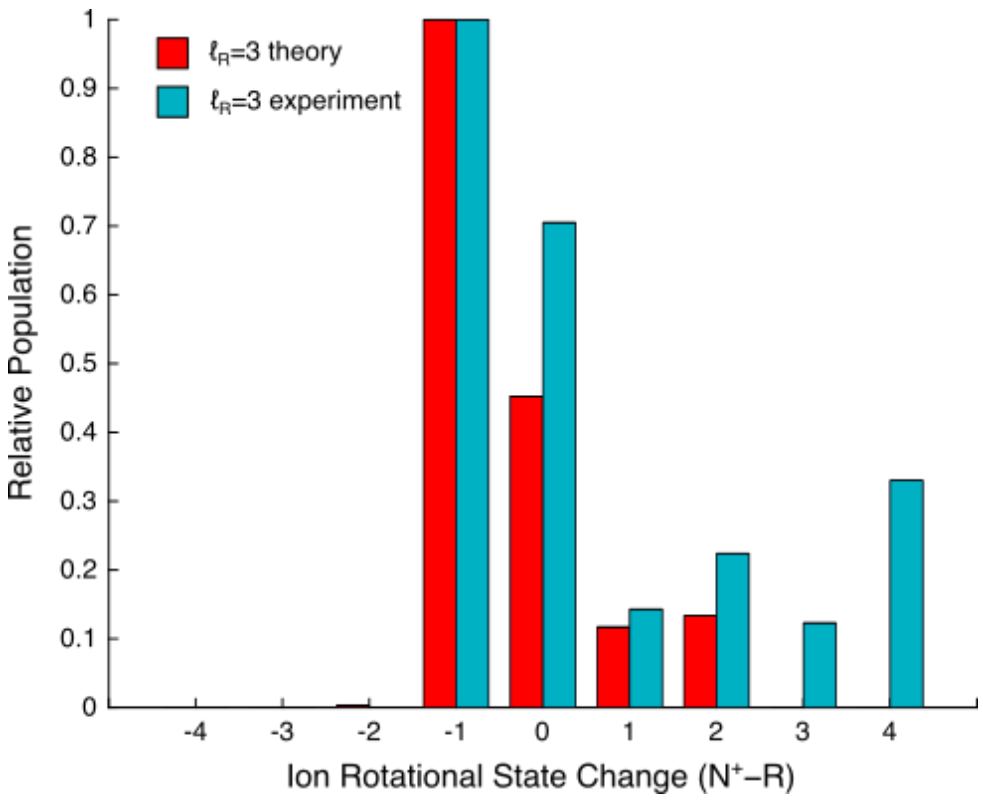

Figure 2. Rotational state change following vibrational autoionization of the 11f (v=2, R=18, ℓR=3) Rydberg state. The experimental data are the B00 values obtained from a fit of the measured photoelectron angular distributions. These values are directly comparable to the rotational state distributions obtained by the model. The intensity pattern for four of the six decay channels is reproduced, but the channels with large rotational state channel are completely absent in the long-range calculation. This suggests an alternate mechanism is responsible for these specific decay pathways.

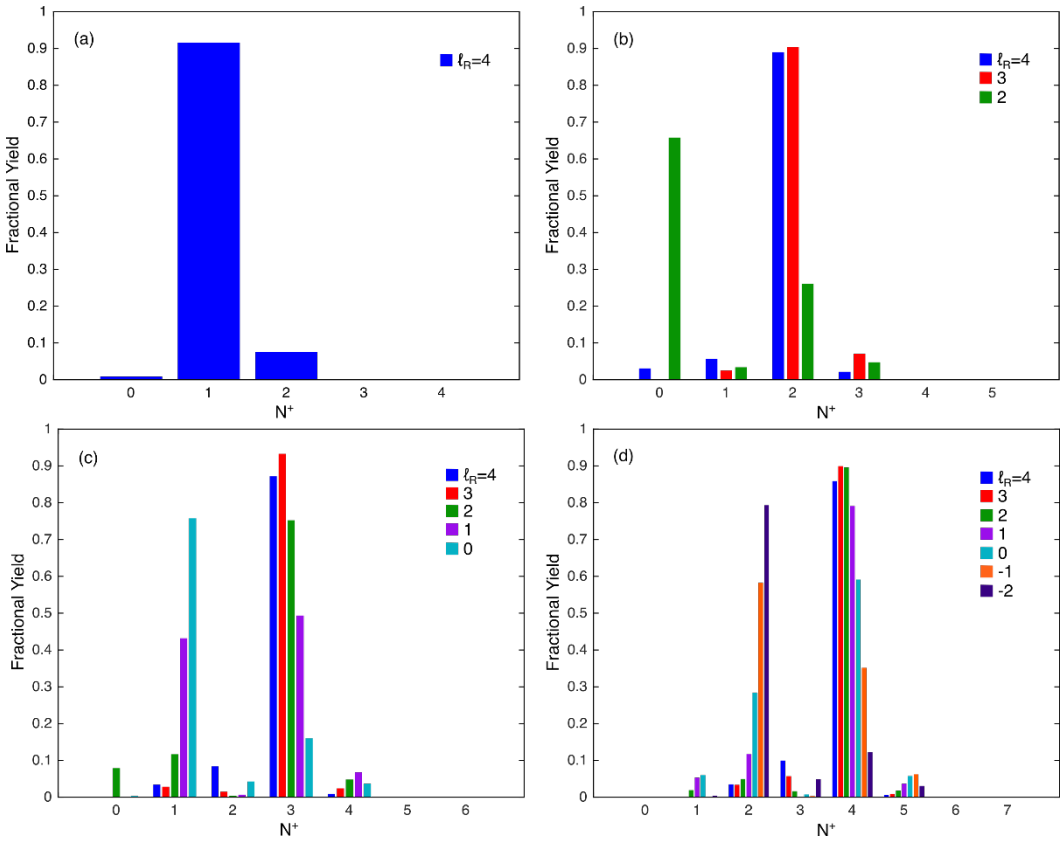

Figure 3. Rotational state distributions of the NO^+ ion following vibrational autoionization of each ℓ_R component of the 25g state with R = (a) 0, (b) 1, (c) 2, and (d) 3. The ℓ_R value is color coded as indicated in the legend of each plot. The dipole mechanism results in decay predominantly via one or both of the N^+–R=±1 channels, dependent on the ℓ_R value.